Climate
of the Past
Open Access

Abrupt shifts of the Sahara–Sahel boundary during Heinrich stadials

J. A. Collins[1,*], **A. Govin**[1], **S. Mulitza**[1], **D. Heslop**[2], **M. Zabel**[1], **J. Hartmann**[3], **U. Röhl**[1], and **G. Wefer**[1]

[1]MARUM – Center for Marine Environmental Sciences and Faculty of Geosciences, University of Bremen,
28359 Bremen, Germany
[2]Research School of Earth Sciences, The Australian National University, Canberra ACT 0200, Australia
[3]Institute for Biogeochemistry and Marine Chemistry, University of Hamburg, Bundesstraße 55, 20146 Hamburg, Germany
[*]now at: Alfred-Wegener-Institut Helmholtz-Zentrum für Polar- und Meeresforschung, Am Alten Hafen 26,
27568 Bremerhaven, Germany

Correspondence to: J. A. Collins (jcollins@awi.de)

Abstract. Relict dune fields that are found as far south as 14° N in the modern-day African Sahel are testament to equatorward expansions of the Sahara desert during the Late Pleistocene. However, the discontinuous nature of dune records means that abrupt millennial-timescale climate events are not always resolved. High-resolution marine core studies have identified Heinrich stadials as the dustiest periods of the last glacial in West Africa although the spatial evolution of dust export on millennial timescales has so far not been investigated. We use the major-element composition of four high-resolution marine sediment cores to reconstruct the spatial extent of Saharan-dust versus river-sediment input to the continental margin from West Africa over the last 60 ka. This allows us to map the position of the sediment composition corresponding to the Sahara–Sahel boundary. Our records indicate that the Sahara–Sahel boundary reached its most southerly position (13° N) during Heinrich stadials and hence suggest that these were the periods when the sand dunes formed at 14° N on the continent. Heinrich stadials are associated with cold North Atlantic sea surface temperatures which appear to have triggered abrupt increases of aridity and wind strength in the Sahel. Our study illustrates the influence of the Atlantic meridional overturning circulation on the position of the Sahara–Sahel boundary and on global atmospheric dust loading.

1 Introduction

Understanding the extent and causes of abrupt millennial-timescale expansions of the Sahara desert is important for the populations of the Sahel region, where dune encroachment causes major problems (FAO, 2010). In addition, constraining the size of the Saharan dust plume is important for determining the role of dust as a climate feedback (e.g. Rosenfeld et al., 2001).

Relict dune fields identified in the modern-day Sahel indicate that during the Late Pleistocene, the Sahara desert and dune-forming conditions were extended further south than today (e.g. Grove, 1958; Talbot, 1980). These relicts which were once active are now stabilised by vegetation (Sarnthein and Diester-Haass, 1977) and are found throughout the semi-arid Sahel (Fig. 1a) as far south as ∼ 14° N (Grove, 1958; Michel, 1973). This is ∼ 5° south of the modern-day boundary of dune formation (at ∼ 19° N in the Western Sahara), which we define as the continental Sahara–Sahel boundary (Fig. 1a) after e.g. Sarnthein and Diester-Haass (1977) and Kocurek et al. (1991). Certain phases of dune mobilisation have been identified (Talbot, 1980), including an "early" phase (> 40 ka; Servant, 1983), the "Ogolian" phase (12–24 ka; Michel, 1973; Servant, 1983; Lancaster et al., 2002), which was the most extensive phase and is often attributed the Last Glacial Maximum (e.g. Talbot, 1980), and a "late" phase following the mid-Holocene (< 5 ka; Swezey, 2001). It has been challenging, however, to determine the

timing of dune formation because of re-mobilisation of dunes during subsequent arid periods, and hence destruction of the record (Kocurek et al., 1991; Chase, 2009). As such, millennial-scale climate changes (such as Heinrich stadial 1; 15–18.5 ka; which occurred within the Ogolian phase) have not been resolved in these continental records. It may be that they have been overprinted during subsequent arid periods or, in the case of Heinrich stadial 1, may not have been distinguished from variations associated with the Last Glacial Maximum.

Pollen from continental records (Lézine, 1989) and a marine core (Dupont and Hooghiemstra, 1989) have also been used to map the continental Sahara–Sahel boundary evolution and also infer an equatorward displacement of $\sim 5°$ latitude at the Last Glacial Maximum. However, these reconstructions also have a relatively low temporal resolution and do not resolve abrupt millennial-scale climate changes. Marine sediments have been used to map the Saharan dust plume, although they have only focussed on certain time slices such as the early or mid-Holocene and the Last Glacial Maximum (Sarnthein et al., 1981; Grousset et al., 1998; Hooghiemstra et al., 2006).

In contrast to sand dune records and the above low-resolution studies, marine sediment cores can provide high-resolution, continuous records of material exported from the continent. Cores from the tropical NE Atlantic between 21° N and 12° N (e.g. Jullien et al., 2007; Mulitza et al., 2008; Tjallingii et al., 2008; Itambi et al., 2009; Zarriess et al., 2011; Just et al., 2012) and from the Mediterranean Sea (Moreno et al., 2002) indicate strong increases in dust export from West Africa during Dansgaard–Oeschger stadials associated with Heinrich events (hereafter referred to as Heinrich stadials, Mulitza et al., 2008). However, the use of different methods prevents a direct comparison of the relative magnitude of variations at each site. Thus, mapping of the spatial evolution of the Sahara desert at high resolution to chart the Sahara–Sahel boundary during these millennial-timescale events has not been performed.

Here, we analyse a transect of four marine cores spanning the Sahara to the Guinea coast (21° N–9° N). By analysing major-element composition using calibrated XRF scanning, a relatively fast technique, we are able to analyse several cores in high resolution. We unmix the sediment in terms of Saharan dust and river-sediment material. This allows us to quantify past changes in dust input, and the associated uncertainty, which is more informative than commonly presented element ratios. Because we analyse the same parameter across four cores, we can directly compare the climate response at different latitudes of the Sahara–Sahel. Furthermore, by interpolating between the cores, we are able to map the spatial (north–south) evolution of dust versus river input to the continental shelf over the last 60 ka. Comparison of our sedimentary records with records of dune formation (which although temporally fragmented are spatially well constrained) suggests that our sedimentary records do

in fact reflect the position of the continental Sahara–Sahel boundary over the last 60 ka. This highlights the importance of Heinrich stadials for dune formation and the position of the Sahara–Sahel boundary.

2 Setting

The continental margin off West Africa receives terrigenous material in the form of two sources: river-suspended sediment and windblown dust. Rivers originate from the humid, high-altitude Fouta Djallon region and enter the ocean between 16° N–5° N (Fig. 1a). The soils of the Fouta Djallon are deeply chemically weathered and are composed mainly of clays (Driessen et al., 2001). As such, river-suspended sediment is relatively enriched in Fe and Al (Supplementary Table 1) and is normally below 10 μm in size throughout the year (Gac and Kane, 1986).

The main source of windblown dust is the Sahara, with a small contribution from the Sahel (Goudie and Middleton, 2001). Most of the dust delivered to the West African margin is blown from the northern Mali–Mauritania region (Fig. 1b) by the winter northeast trade winds (Sarnthein et al., 1981; Bory and Newton, 2000; Skonieczny et al., 2011). Some dust is also entrained into the Saharan Air Layer by convective summer storms and travels further, with part reaching the Caribbean (Prospero et al., 1981). Dust originates from arid regions, which, for the major source regions, have remained relatively arid during most of the Pleistocene (deMenocal, 1995). Therefore, compared to river sediment, dust is relatively enriched in Si (Supplementary Table 1) and is normally larger (size greater than 10 μm; Stuut et al., 2005). This is mostly due to higher content of quartz grains in dust (Moreno et al., 2006) relative to river material. At the coast, the dust plume spans approximately 25° N–15° N, centred at $\sim 20°$ N (Fig. 1b). As such, this results in a Si-rich dust source located to the north of the Al- and Fe-rich fluvial source region. The north–south gradient between the two sources of material is reflected in the major-element composition of continental margin surface sediments (Govin et al., 2012; Fig. 1c), with the highest Si/Al ratios in the northernmost, dust-dominated part of our study region.

Surface ocean currents in this region (Fig. 1a) include the southward-flowing Canary Current, its coastal arm the African Coastal Current, the northward-flowing coastal Mauritania Current and the North Equatorial Countercurrent (e.g. Mittelstaedt, 1983). The two coastal currents oscillate along with the trade winds, with the southward-flowing component dominant in winter and the northward component dominant in summer. Intermediate currents in this region are dominated by the northward-flowing Antarctic Intermediate Water and a southward-flowing Mediterranean Intermediate water. Modern bottom currents are dominated by the southward-flowing North Atlantic Deep Water.

Table 1. Sediment core transect.

Core Label	Core Number	Latitude	Longitude	Water Depth (m)	Age model based on	Age model reference
1	GeoB7920-2	20°45.09′ N	18°34.90′ W	2278	^{14}C, δ^{18}O	Tjallingii et al. (2008); Collins et al. (2011)
2	GeoB9508-5	15°29.90′ N	17°56.88′ W	2384	^{14}C, δ^{18}O	Mulitza et al. (2008)
3	GeoB9526-5	12°26.10′ N	18°03.40′ W	3223	^{14}C, δ^{18}O	Zarriess and Mackensen (2010); Zarriess et al. (2011)
4	GeoB9528-3	09°09.96′ N	17°39.81′ W	3057	δ^{18}O	Castañeda et al. (2009)

3   Methods

We use four sediment cores (Table 1) spanning from 21° N to 9° N off West Africa (Fig. 1) covering the gradient between dust and river sources. Sediment core chronology is based on published age models (see Table 1 for references) using both radiocarbon and benthic foraminiferal δ^{18}O correlation.

Sediment major-element composition was measured using the Avaatech X-ray fluorescence core scanner at MARUM, University of Bremen (Cores 1 and 2; Bloemsma et al., 2012 and Core 4; this study) and at Alfred Wegener Institute, Bremerhaven (Core 3; Zarriess and Mackensen, 2010; Zarriess et al., 2011). XRF scanner elemental intensities were calibrated to elemental concentrations (Weltje and Tjallingii, 2008) by regression with at least 50 discrete powder samples from each core (Core 1; Bloemsma et al., 2012; Core 2; Mulitza et al., 2008; Cores 3 and 4; this study), which were quantified using EDP-XRF spectroscopy at MARUM, University of Bremen. The robustness of the calibration is indicated as the fit of the calibrated scanner data with the discrete powder samples (Supplementary Fig. 1).

Commonly, major-element data are presented as elemental ratios (e.g. Mulitza et al., 2008; Zarriess et al., 2011). Rather than interpreting elemental ratios, we directly quantify the major element data in terms of the relative proportion of Saharan dust, river-suspended material and marine-derived material by using an endmember unmixing analysis. Details of this analysis are given in Mulitza et al. (2010). Briefly, representative "dust" and "river" endmember major-element compositions were estimated using a bootstrap with replacement routine (500 iterations) based on the relative proportions of Al, Si, Fe, K, Ti and Ca from 28 Sahara–Sahel dust and soil samples and 10 Senegal River suspension samples taken from close to the river mouth (Supplementary Table 1). For the dust endmember, by considering aeolian material from a range of geographical regions and constructing spectra of endmember compositions via bootstrapping (Mulitza et al., 2010), the variability due to the possibility of shifting source areas is incorporated into the uncertainty of the unmixing results. The composition of the marine component (Ca and Si; Supplementary Table 1) was estimated based on biogenic silica content (Collins et al., 2011) and measured Ca con-

centration, and was held constant downcore (after Mulitza et al., 2010). The contribution of Si from biogenic opal is low (< 3.5 wt% SiO_2), and downcore variations between major climate regimes (e.g. modern-day, Last Glacial Maximum and Heinrich stadial 1) are small. Error on the marine end-member composition (Supplementary Table 1) was nonetheless integrated into the unmixing analysis and propagated into the final uncertainty on the dust% estimates. We represent the data as dust%, where dust% = 100*dust/(river + dust). Dust% is the median value of the 500 bootstrap iterations, and uncertainty is represented as non-parametric 68% (1σ) confidence intervals (16th and 84th percentiles) of the iterations. Because of the difficulty of constraining the sedimentation rate of individual millennial-scale events (Just et al., 2012), we do not estimate dust accumulation rates.

To determine the modern-day dust% value in the sediment at the latitude of the Sahara–Sahel boundary (19° N), we performed a robust linear regression between latitude and dust% for the late Holocene sections (defined as the mean of the core-top sediment down to an age of 3 ka) of our cores (Fig. 1c) and for the surface sediments of Govin et al. (2012). We calculate a mean value for the late Holocene because the core-top does not always correspond to the present day, due to loss of uppermost sediments during coring. We include dust% calculated for the more extensive compositional data set of Govin et al. (2012) between 26° N and 3° N to further verify the spatial pattern of dust% and to assess the compositional scatter of continental margin sediments. The compositional scatter is incorporated into the uncertainty on the regression, which is represented as 68 % (1σ) confidence intervals.

To determine the position of the Sahara–Sahel boundary over time, we linearly interpolated each of the four sediment-core dust% time series into time steps of 250 yr. For each time step, we performed a robust linear regression between dust% and latitude and solved the equation to calculate the latitude corresponding to the modern-day Sahara–Sahel boundary dust% value. Propagated uncertainties include the following: uncertainty on the endmember composition, uncertainty on the dust% value at the modern-day sedimentary Sahara–Sahel boundary (Fig. 1c) and uncertainty on the linear regression for the past time steps (based on 68 %
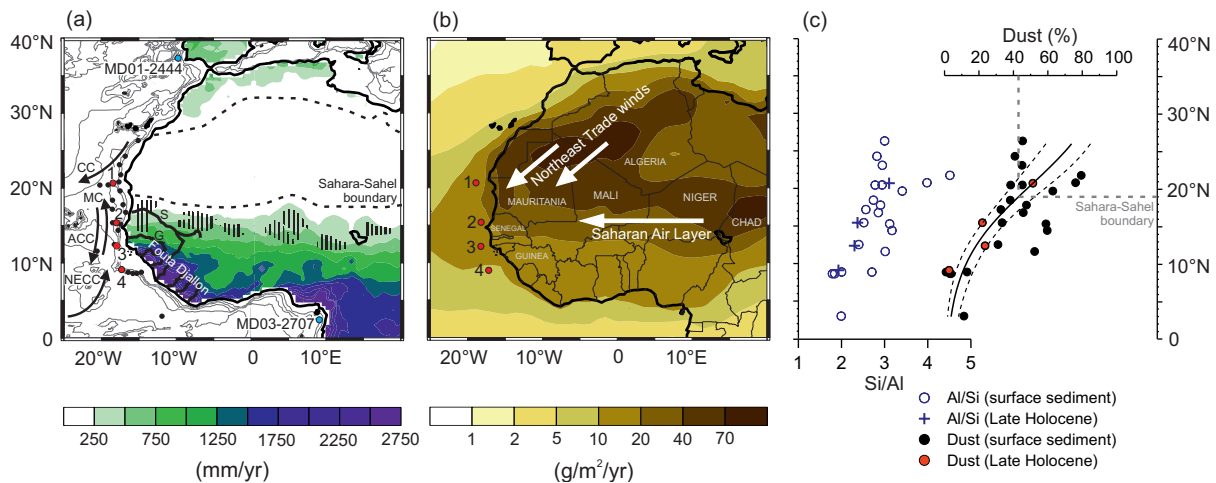
Fig. 1. (a) Annual-mean rainfall $(mm\,yr^{-1})$ for West Africa from the University of Delaware precipitation data set (climate.geog.udel.edu/~climate; average for 1950–1999). Thick black lines highlight the main African rivers of the study area: the Senegal River (S), Gambia River (G) as well as numerous small rivers draining the Fouta Djallon. Hatching marks the approximate position of relict sand dunes in the Sahel, re-drawn after Grove (1958). Black dotted lines mark the approximate boundaries of modern-day dune formation (Sarnthein and Diester-Haass, 1977) – the southern one is the continental Sahara–Sahel boundary. Red dots mark locations of Cores 1–4 (see Table 1). Blue dots mark the locations of cores MD01-2444 (Martrat et al., 2007) and MD03-2707 (Weldeab et al., 2007). Black dots mark locations of surface samples (Govin et al., 2012) plotted in Fig. 1c. Black arrows mark surface currents: Canary Current (CC), African Coastal Current (ACC), Mauritania Current (MC) and North Equatorial Countercurrent (NECC). **(b)** Modern-day dust deposition $(g\,m^2\,yr^{-1})$ for West Africa (Mahowald et al., 2005), highlighting the Saharan dust plume. **(c)** Si/Al (blue) and dust% (black and red) of surface sediments (Govin et al., 2012) and late Holocene section of Cores 1–4. Solid line represents robust linear regression between latitude and dust% (plot is rotated 90°) for samples covering the gradient between dust and river material (26° N–3° N). Data have been transformed as log ((100-dust%)/dust%) so that the regression lies in the interval (0, 100). The correlation (r^2) is 0.51. Black dashed lines represent 68% (1σ) confidence intervals, which equates to on average ±9 % dust. Grey dashed line represents the interception of the modern-day continental Sahara–Sahel boundary position (19° N) with the regression line, at 43 % dust.

confidence intervals on the regression). Examples of the linear regression for past time steps from a range of climate states are given (Supplementary Fig. 2).

4 Results

For the late Holocene section (last 3 ka to core top) of the sediment cores, dust% values decrease from north to south, e.g. from 51 % at Core 1 (21° N) to 3 % at Core 4 (9° N; Fig. 1c). These values are in good agreement with those based on the surface sediments (Fig. 1c; Govin et al., 2012). At the latitude of the modern-day continental Sahara–Sahel boundary (19° N), the regression between latitude and dust yields a dust% value of 43 %. The uncertainty on this value associated with the compositional scatter is ±9 % (Fig. 1c).

Dust% values in Cores 1–4 exhibit a similar evolution to each other over the last 60 ka (Fig. 2). Dust% is closely correlated to the Si/Al ratios (Fig. 1c, Supplementary Fig. 3); these elements differ strongly between the dust and river endmembers (Supplementary Table 1). Si is associated with coarse windblown quartz grains while Al is associated with fine river clays. Consequently dust% and Si/Al are closely correlated to grain size and mineralogy (Mulitza et al., 2008).

The main features over time are increases in dust% during Heinrich stadials 1 (15–18.5 ka), 2 (23.5–25.5 ka), 3 (29–30.5 ka), 4 (38.5–40 ka) and 5 (47–48.5 ka). These increases in dust are strongest in Cores 2 and 3, probably because they are positioned in the transition zone between dust- and river-dominated regions and hence are most sensitive to changes in the position of the Sahara–Sahel boundary. There is also a gradual trend of increasing dust% from 60 ka to the Last Glacial Maximum (19–23 ka) in Cores 1–3. In Cores 1 and 2, dust values decrease during the Bølling–Allerød (14.7–12.9 ka) and increase during the Younger Dryas (12.9–11.6 ka). In Cores 2 to 4, dust% values are lowest during the Holocene (Fig. 2c–e).

The interpolated latitudinal position of the 43 ± 9 % dust value (the sedimentary Sahara–Sahel boundary) is plotted in Fig. 3d and follows a similar pattern to dust% values of the individual Cores 1–4. Over time, the sedimentary Sahara–Sahel boundary reaches its southernmost position (13° N ± 3°) during Heinrich stadials 1, 2, 4 and 5. It reaches 15° N ± 3° at the Last Glacial Maximum and 16° N ± 3° during Heinrich stadial 3. It reaches its northernmost position (21° N ± 5°) during the mid-Holocene (~ 6 ka) and at ~ 51 ka (Fig. 3d).
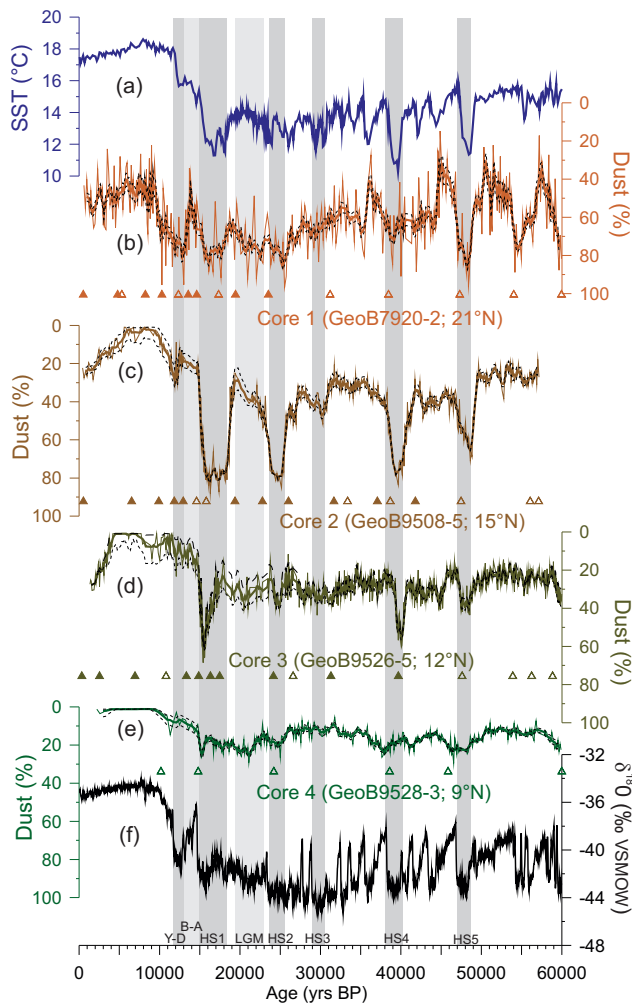
Fig. 2. Records of dust% from the West African margin compared with NE Atlantic sea surface temperature and Greenland Ice Core δ^{18}O. **(a)** Sea surface temperature of the Iberian margin (Core MD01-2444; 38° N; Martrat et al., 2007). **(b–e)** Dust% values for Core 1 (GeoB7920-2, 21°N), Core 2 (GeoB9508-5; 15°N), Core 3 (GeoB9526-5; 12° N) and Core 4 (GeoB9528-3; 9° N). Note that y-axes are inverted. Solid line is the median of 500 iterations. Thick line represents five-point running average. Uncertainty (black dashed lines) includes the following: uncertainty on dust and river endmember compositions (based on 16th and 84th percentiles of 500 iterations) and uncertainty on marine component (based on variations in opal content). Grey bars highlight Heinrich stadials (HS), Last Glacial Maximum (LGM), Younger Dryas (Y-D), and Bølling–Allerød (B-A). Timing is based on the Dansgaard–Oeschger stadials in Greenland ice (Fig. 2f; Svensson et al., 2008). **(f)** δ^{18}O of Greenland ice (NGRIP, 2004, Svensson et al., 2008; five-point running average). Filled triangles indicate AMS radiocarbon ages. Open triangles indicate tie-points derived from benthic foraminiferal δ^{18}O correlation (see Table 1 for references).
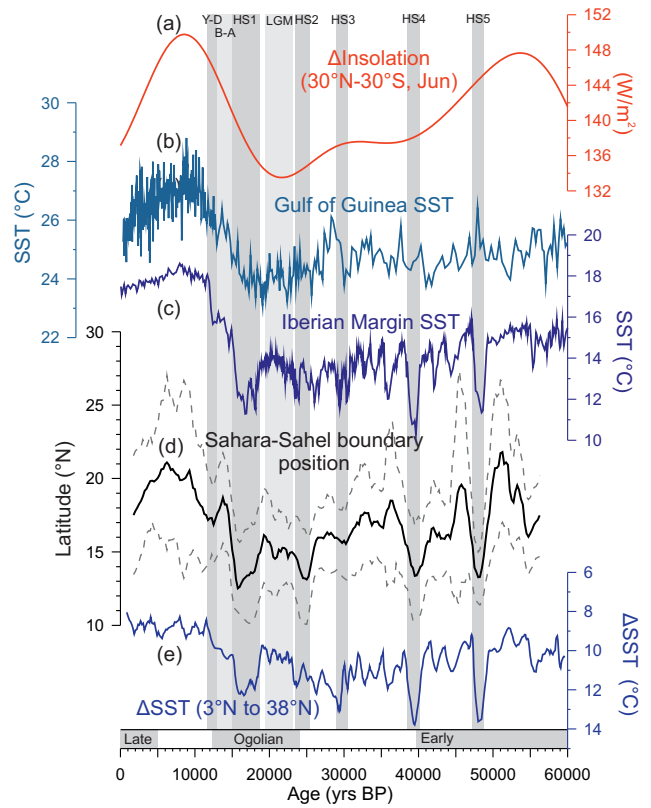
Fig. 3. (a) Boreal summer (July-August-September) insolation difference between 30° N and 30° S. **(b)** Sea surface temperature of the Gulf of Guinea (MD03-2707; 3° N; Weldeab et al, 2007). **(c)** Sea surface temperature of the Iberian margin (MD01-2444; 38° N; Martrat et al., 2007). **(d)** Latitudinal position of the sedimentary Sahara–Sahel boundary (43 % dust value) over the last 60 ka. Thick line represents a five-point (1 ka) running average. Uncertainty (grey dashed lines) includes the following: uncertainty on the endmember compositions (as in Fig. 2), uncertainty on modern-day dust% at the Sahara–Sahel boundary (based on 68% confidence intervals; Fig. 1c) and uncertainty on the regression for past time steps (68% confidence intervals; examples are given in Fig. SF2). **(e)** Sea surface temperature difference (five-point running average) between the Iberian margin (38° N; Martrat et al., 2007) and the Gulf of Guinea (3° N; Weldeab et al., 2007). Vertical grey bars are as in Fig. 2. The early, Ogolian and late phases of dune formation are marked.

5 Discussion

5.1 Oceanic controls on past sediment composition

The gradient in dust from 26° N to 3° N for the surface sediments and the late Holocene section of the cores (Fig. 1c) suggests that dust% reflects input from the adjacent continent (Fig. 1a, b). However, the absolute values of dust% from sediments adjacent to the dust-dominated region appear rather low (e.g. 51 % at Core 1; Fig. 2b). Nonetheless, this value is comparable with estimates of dust% based on grain-size data

(Tjallingii et al., 2008), suggesting it is not due to mischaracterisation of our dust and river endmembers. Instead, because river-derived material is generally finer than dust (Stuut et al., 2005; Gac and Kane, 1986), it is likely to be due to grain-size sorting processes during sediment transport. Specifically, the low dust% values are thought to be due to lateral ocean advection and aggradation of the river endmember (Tjallingii et al., 2008). This suggests that sediments may be generally slightly biased towards the river endmember, relative to the material exported from the adjacent continent.

Ocean currents can act to re-work and partition the sediment on the shelf and slope as seen today (e.g. Michel et al., 2009). These processes likely explain some of the compositional scatter between modern-day sediments (Fig. 1c). The uncertainty on the modern-day Sahara–Sahel boundary composition (± 9 % dust) from this scatter is taken into account in our reconstruction of past Sahara–Sahel boundary position. Over time, these processes may explain some of the small differences in the evolution between the four records (Fig. 2b–e). However, we suggest that over the course of the last 60 ka, ocean currents are unlikely to be the main control on the large-scale consistent patterns between our records and on the position of the sedimentary Sahara–Sahel boundary. Ocean currents would probably only affect the fine (i.e. river-derived) fraction of the sediment because the coarser (dust) fraction sinks too rapidly to be transported any great distance by ocean currents (Grousset et al., 1998; Wefer and Fischer, 1993). Past changes in current speeds are not well known. If, however, the Canary Current or African Coastal Current were enhanced during Heinrich stadials, fine (river-derived) material that is today carried north from the Senegal would have been likely carried south. Similarly, fine material that is today carried south would have been advected further southwards. As such, we would expect a general southwards transport of material and hence a relative increase in river material (i.e. a decrease in dust%) in the southern cores, particularly in Cores 3 and 4, which are south of the Senegal River. However, this is not the pattern displayed by our data. Over most of the last 60 ka, we see the same response at each of our core sites (for example increases in dust% at all sites during Heinrich stadials), suggesting that changes in a given current are unlikely to be the major controlling factor on our dust%. Increases in dust% at all core sites might be explainable by complete removal of fine material from the entire West African margin between 21° N and 9° N. However, such a scenario, requiring extreme current speeds along the entire margin, seems unrealistic. Bottom currents during Heinrich stadials are thought to have switched from the southward-flowing North Atlantic Deep Water to the northward-flowing Antarctic Intermediate Water. Again, however, we see no northward shift in the distribution of fine river-derived material in our dust% data. It seems more likely that if the northward flow of the Antarctic Bottom Water was significant, it likely acted to counteract the effect of any increase in southward-flowing surface currents.

The four cores are from a similar water depth (2278–3223 m) and so any grain-size fractionation associated with transport distance from shore to core site should be similar between cores. Moreover, any effect of differences in water depth should also be incorporated in the uncertainty on the composition of the modern-day Sahara–Sahel boundary composition (± 9 % dust). Just et al. (2012) suggested that reduced sea level during the glacial, which decreased the distance between river mouths and the core site, acted to increase the contribution of river material to their sediment core. However, in our cores, we see no systematic increase in river material during the glacial period, when sea level was lower. Another marine sediment core study (Jullien et al., 2007), which is located on a seamount further away from the coast (and thus is expected to be less susceptible to sea-level changes), also displays increased dust input during the glacial relative to the Holocene, and is thus in agreement with our data. Exposure of the shelf during sea-level lowstands would have contributed an additional source of dust because dunes migrated onto the shelf (Sarnthein and Diester-Haass, 1977). Hence the dust source would have also shifted closer to the core site. As such, perhaps there is little influence of sea level in our cores because the distance to both sources decreased (i.e. distance to dust source *and* distance to river mouth).

It has been suggested that coarse dust-like material during Heinrich stadials might have been delivered to the core sites as turbidity currents (Sarnthein and Diester-Haass, 1977). Turbidites are indeed a common occurrence in sediments from this region, particularly in canyon settings and are the main oceanographic method of transporting coarse material from the shelf to the slope and deep sea (Hanebuth and Henrich, 2009; Henrich et al., 2010; Pierau et al., 2011). However, these studies do not document a systematic increase in turbidity current activity at the time of Heinrich stadials. As such it is hard to reconcile that increased dust% during Heinrich stadials in our cores, which are not from canyons, would be due to turbidity currents. In addition, typical deep-water benthic foraminiferal δ^{18}O values during Heinrich stadials from Core 2 (Mulitza et al., 2008) suggest autochthonous calcification and deposition rather than downslope transport from shallower and warmer water masses. Similarly the grain size data do not show a typical fining-upwards sequence (Mulitza et al., 2008) as seen in typical turbidites from this region (Henrich et al., 2010). Thus, we suggest that the increase in dust-like material during Heinrich stadials could not have been delivered to the core site as turbidity currents originating from the upper slope, but was rather delivered as windblown dust.

Overall, we suggest that shifts in the sedimentary Sahara–Sahel boundary are mainly due to continental changes in dust export and the position of the continental Sahara–Sahel boundary rather than oceanographic processes. Specifically, sand dunes (i.e. the continental Sahara–Sahel boundary) were forming as far south as $\sim 14°$ N (Fig. 1a) in Senegal and

Chad during glacial times (Grove, 1958; Michel, 1973; Servant, 1983), a similar latitude to the southernmost position of the sedimentary Sahara–Sahel boundary (Fig. 3d). Below (Sect. 5.3) we argue that these periods of dune formation on the continent were coeval with Heinrich stadials.

5.2 Dune formation and dust mobilisation

Both dust mobilisation and sand dune formation are a function of vegetation cover (aridity), sediment supply and wind strength (Sarnthein and Diester-Haass, 1977; Prospero and Lamb, 2003; Pye, 1989; Chase, 2009). Decreased vegetation coverage permits mobilisation of sand dunes and deflation of dust. However, since both processes also require supply of material, arid (rather than hyper-arid) conditions are thought to provide optimal conditions (Rea, 1994). Intermittent wet and dry periods may act to replenish and deflate dust sources, respectively (McTainsh, 1987). Although sand dunes are normally too coarse to be deflated by wind, fine material formed by in situ weathering during semi-arid phases may be deflated as dust during subsequent arid phases and dune re-activation (Pye, 1995). We suggest that aridification of the Sahel during Heinrich stadials (Niedermeyer et al., 2010) exposed new dust sources of material, which were deflated and contributed to dune formation. Although Sahelian dust sources are more chemically weathered than those in the Sahara (Stuut et al., 2005), they are still much less weathered than the river-derived endmember sourced from the Fouta Djallon (Gac and Kane, 1986; see also soil maps of Driessen et al., 2001). In addition to dust mobilisation, aridity also controls the input of river sediment discharge, with greater discharge during less arid periods (Gac and Kane, 1986; Coynel et al., 2005). As such, reduced precipitation would have simultaneously acted to reduce input of river material and increase input of dust material. It might be possible that increased precipitation in arid regions would have increased river strength and hence increased river input of coarse material. However, this is unlikely to be the cause of increased dust% during Heinrich stadials because hydrological proxies (Niedermeyer et al., 2010) and climate models (Mulitza et al., 2008) indicate drier rather than wetter conditions during Heinrich stadials.

As well as aridity and sediment supply, another important factor controlling both dust export and dune formation is wind strength (Sarnthein and Diester-Haass, 1977; Talbot, 1980). Northeast trade winds are thought to have been stronger at the Last Glacial Maximum (Sarnthein et al., 1981). During Heinrich stadials they were likely stronger still, as implied by the increase in the grain size of the coarse dust endmember (Mulitza et al., 2008). Stronger winds may have also acted to deflate new dust sources that were previously too coarse to be deflated. It is possible that a stronger dust plume associated with stronger winds would have increased dust input and hence controlled the position of the sedimentary Sahara–Sahel boundary inde-

pendently from the position of the continental Sahara–Sahel boundary. However, we suggest that wind strength cannot be the sole control on the sedimentary Sahara–Sahel boundary because of the latitudinal position of continental dunes, which act as markers for the past position of the continental Sahara–Sahel boundary.

Changes in wind direction might also be expected to control the trajectory of the dust plume and thus could also control the latitudinal position of the sedimentary Sahara–Sahel boundary independently of the continental Sahara–Sahel boundary. However, dune trends in Mauritania dated between 15–25 ka indicate a more zonal wind trajectory (NE–SW) compared to today (N–S; Lancaster et al., 2002). In fact, most relict dunes from other regions also display a (NE–SW) trajectory (Grove and Warren, 1968; Talbot, 1980). As such, the observed equatorward shifts of the sedimentary Sahara–Sahel boundary during the glacial relative to today (Fig. 3d) cannot be attributed to a more meridional wind direction. Therefore, we suggest that shifts in the sedimentary Sahara–Sahel boundary are mainly due to shifts in position of the continental Sahara–Sahel boundary.

5.3 Timing of dune formation

The main episode of dune formation, when dunes reached $14°$ N, was the Ogolian phase, which has been dated at 15–24 ka in Mauritania (Lancaster et al., 2002), and slightly later, at 20–12 ka, in Senegal (Michel, 1973) and Chad (Servant, 1983). The Ogolian phase is commonly associated with Last Glacial Maximum conditions (e.g. Talbot, 1980). Our data indicate that the sedimentary Sahara–Sahel boundary was positioned at $15°$ N $\pm 3°$ at the Last Glacial Maximum (19–23 ka), which is also in agreement with estimates from pollen-based studies (Dupont and Hooghiemstra, 1989; Lézine, 1989), and was positioned at $13°$ N $\pm 3°$ during Heinrich stadial 1 (15–18.5 ka). Considering that the glacial dust plume was stronger than today (Sarnthein et al., 1981), it is unlikely that the continental dunes could have reached $14°$ N while the sedimentary Sahara–Sahel boundary was located further to the north ($15°$ N). As such, we suggest that the southernmost dunes formed when the sedimentary Sahara Sahel boundary was at $13°$ N $\pm 3°$ rather than at $15°$ N $\pm 3°$, i.e. at Heinrich stadial 1 rather than the Last Glacial Maximum. Morphological studies have suggested the path of the Senegal River was obstructed by shifting dunes during the Ogolian period (Michel, 1973). Again, based on our data it seems likely that this took place, or was most severe, during Heinrich stadial 1.

Another dune building phase at $14°$ N, the early phase (Fig. 3), has been dated at > 40 ka (Servant, 1983). During Heinrich stadial 4 (38.5–40 ka) and Heinrich stadial 5 (47–48.5 ka), the sedimentary Sahara–Sahel boundary was also located at a latitude of $13°$ N $\pm 3°$ (Fig. 3d). This represents a shift of at least $7° \pm 6°$ latitude from the background glacial

state at this time. As such, we suggest that dunes at 14° N were likely formed during Heinrich stadial 4 and 5.

5.4 Global climate teleconnections

The Sahara–Sahel boundary exhibits a gradual equatorward shift from 60 ka to the Last Glacial Maximum (Fig. 3d). This may be a product of the gradual reduction in July-August-September cross-equatorial insolation gradient (Fig. 3a), as has been proposed (Zarriess et al., 2011). A reduced insolation gradient is expected to have reduced the northward penetration of the summer monsoon, and caused an equatorward shift of the continental Sahara–Sahel boundary. The gradual equatorward Sahara–Sahel boundary shift may also be partly attributable to the increasing severity of glacial conditions from 60 ka to the Last Glacial Maximum and the associated increases in aridity and wind strength on the continent (Sarnthein et al., 1981). Conversely, during the mid-Holocene, an increased July-August-September cross-equatorial insolation gradient induced greater northward penetration of the West African monsoon (e.g. Kutzbach and Liu, 1997) and would have increased vegetation coverage in the Sahel and Sahara, shifting the Sahara–Sahel boundary northwards and reducing the area of dust mobilisation and dune formation (e.g. Salzmann and Waller, 1998; Watrin et al., 2009). Our estimate of Sahara–Sahel boundary position during the mid-Holocene (21° N ± 3°) is in broad agreement with estimates determined from plant community distribution (23° N; Watrin et al., 2009). The increase in dust% (Figs. 2b–d) and southward shift of the Sahara–Sahel boundary (Fig. 3d) from the mid- to late Holocene was relatively minor compared to the rest of our record. This is in line with dune records suggesting that the "late" phase of sand dune formation (Fig. 3) was associated with relatively minor mobilisation of sand (Talbot, 1980). Finally, during the transition from the mid- to late Holocene, none of our records display an abrupt increase in dust (Figs. 2b–e, 3d) as seen in another record (deMenocal et al., 2000). Our data thus suggest a gradual response to decreasing summer insolation during this period in contrast to previous interpretations (deMenocal et al., 2000).

Our data display abrupt changes in Sahara–Sahel boundary position during Heinrich stadials. These appear to be the result of a sharp decrease in North Atlantic, and particularly, Iberian margin, sea surface temperatures (Figs. 2a, 3c; e.g. Cortijo et al., 1997; de Abreu et al., 2003; Martrat et al., 2007; Eynaud et al., 2009; Kageyama et al., 2009; Salgueiro et al., 2010). This cooling is thought to have been due to slowdown of the Atlantic meridional overturning circulation and reduced deep-water production during Heinrich stadials (e.g. McManus et al., 2004). The cooling was manifested as equatorward shifts of the polar front as far south as the Iberian margin (Eynaud et al., 2009). The magnitude of sea surface temperature changes during Heinrich stadials appears to be closely coupled to shifts of the Sahara–Sahel boundary. For example, the coolest sea surface temperatures (Heinrich

stadials 1, 4 and 5; Fig. 3c) and the most intense equatorward shifts of the polar front (Eynaud et al., 2009) resulted in the largest equatorward Sahara–Sahel boundary shifts (Fig. 3d). Heinrich stadial 2 is slightly anomalous in this regard (most records show small magnitude cooling) although there is a larger cooling at Heinrich stadial 2 in the record of Cortijo et al. (1997). Also, in the record from Martrat et al. (2007), Heinrich stadial 4 is anomalously cool compared to other records.

Sea surface temperature is linked to the position of the Sahara–Sahel boundary via its control on precipitation and wind strength. The marked cooling in the North Atlantic is thought to have increased the strength of the African Easterly Jet, which led to reduced precipitation in the Sahel (Mulitza et al., 2008; Niedermeyer et al., 2010; Bouimetarhan et al., 2012). This would have activated dunes and engendered dust mobilisation from the Sahel, shifting the Sahara–Sahel boundary to the south. Trade-wind strength, on the other hand, is thought to be controlled by the meridional sea surface temperature gradient (e.g. Kim et al., 2003). Therefore, we suggest that the sea surface temperature difference between the Iberian margin (Fig. 3c, Martrat et al., 2007) and the Gulf of Guinea (Fig. 3b, Weldeab et al., 2007), which was greater by up to 4 °C during Heinrich stadials (Fig. 3e), mainly due to cooling off Iberia, acted to increase the strength of the northeast trade winds and thus the "strength" of the dust plume.

The position of the Sahara–Sahel boundary was shifted equatorward to 17° N ± 2° at the Y-D (Fig. 3d), which is in line with increased dune activity in Mauritania at ∼ 19° N at this time (Lancaster et al., 2002). In most records, there is a relatively small sea surface temperature decrease in the northeast Atlantic (Fig. 3c), although cooling in the northern high latitudes was relatively large (Fig. 2f). This therefore suggests a different mechanism of transmission compared to Heinrich stadials, perhaps via an atmospheric teleconnection.

The response of the position of the Sahara–Sahel boundary to changes in sea surface temperature was rapid, both equatorward and poleward (Fig. 3d). All cores responded coevally indicating a very rapid expansion and retreat of the Sahara–Sahel boundary. At Heinrich stadial 5 for example, the Sahara–Sahel boundary migrated 7° south and 7° north in 4 ka, equivalent to a rate of approximately 400 m yr^{-1} (Fig. 3d). This may represent southward migration of sand dunes or re-activation of existing dunes. If it represents dune migration, it is at least an order of magnitude greater than modern estimates of dune migration rate: 7.5 m yr^{-1} for barchan dunes in NW Sudan (Haynes Jr., 1989) and between 0.17 and 30 m yr^{-1} for other regions (Marín et al., 2005; Bristow et al., 2005; Muckersie and Shepherd, 1995). The speed of dune migration/re-activation highlights the potential for dune re-activation and increased dust export during a future precipitation decrease in the western Sahel (Meehl et al., 2007).

Finally, our data suggest that the dust plume was stronger and was 6° wider during Heinrich stadials 1, 2, 4 and 5 relative to today, which would have increased global atmospheric dust loading. The magnitude of feedbacks from such an increase in atmospheric dust loading requires further investigation, in particular regarding its contribution to the cooling (Miller and Tegen, 1998) and aridity (Rosenfeld et al., 2001) of Heinrich stadials.

6 Conclusions

We have presented a high-resolution record of the position of the Sahara–Sahel boundary over the last 60 ka based on an estimation of the dust- versus river-derived material (dust%) in hemipelagic sediments retrieved from a latitudinal transect of cores off West Africa. Our data indicate that sediments composed of $43\% \pm 9\%$ dust, equivalent to those at the modern-day Sahara–Sahel boundary (19° N), were present down to a latitude of $13°$ N $\pm 3°$ during Heinrich stadials 1, 2, 4 and 5, an equatorward shift of around 6° relative to the modern day. Relict sand dunes at 14° N latitude on the continent imply that the southward shifts of the sedimentary Sahara–Sahel boundary must reflect shifts of the continental Sahara–Sahel boundary. We find that the largest and most abrupt equatorward shifts of the Sahara–Sahel boundary position, during Heinrich stadials, were likely induced by extremely cold North Atlantic sea surface temperatures, which would have increased Sahel aridity and trade wind strength, thus mobilising dust and activating sand dunes. Our study highlights the importance of millennial-timescale changes in the Atlantic meridional overturning circulation for the position of the Sahara–Sahel boundary and for global atmospheric dust loading.

Supplementary material related to this article is available online at: http://www.clim-past.net/9/1181/2013/cp-9-1181-2013-supplement.pdf.

References

Bloemsma, M. R., Zabel, M., Stuut, J-B. W., Tjallingii, R., Collins, J. A., and Weltje, G. J.: Modelling the joint variability of grain size and chemical composition in sediments, Sediment. Geol., 280, 135–148, 2012.

Bory, A. J. M. and Newton, P. P.: Transport of airborne lithogenic material down through the water column in two contrasting regions of the eastern subtropical North Atlantic Ocean, Global Biogeochem. Cy., 14, 297–315, 2000.

Bouimetarhan, I., Prange, M., Schefuß, E., Dupont, L., Lippold, J., Mulitza, S., and Zonneveld, K.: Sahel megadrought during Heinrich Stadial 1: evidence for a three-phase evolution of the low- and mid-level West African wind system, Quaternary Sci. Rev., 58, 66–76, 2012.

Bristow, C. S., Lancaster, N., and Duller, G. A. T.: Combining ground penetrating radar surveys and optical dating to determine dune migration in Namibia, J. Geol. Soc., 162, 315–321, 2005.

Castañeda, I. S., Mulitza, S., Schefuß, E., Lopes dos Santos, R. A., Sinninghe Damsté, J. S., and Schouten, S.: Wet phases in the Sahara/Sahel region and human migration patterns in North Africa, Proc. Natl. Acad. Sci. USA, 106, 20159–20163, 2009.

Chase, B. M.: Evaluating the use of dunes sediments as a proxy for palaeo-aridity: A southern African case study, Earth-Sci. Rev., 93, 31–45, 2009.

Collins, J. A., Schefuß, E., Heslop, D., Mulitza, S., Prange, M., Zabel, M., Tjallingii, R., Dokken, T. M., Huang, E., Mackensen, A., Schulz, M., Tian, J., Zarriess, M., and Wefer, G.: Interhemispheric symmetry of the tropical African rainbelt over the past 23,000 years, Nat. Geosci., 4, 42–45, 2011.

Cortijo, E., Labeyrie, L., Vidal, L., Vautravers, M., Chapman, M., Duplessy, J.-C., Elliot, M., Arnold, M., Turon, J.-L., and Auffret, G.: Changes in sea surface hydrology associated with Heinrich event 4 in the North Atlantic Ocean between 40° and 60° N, Earth Planet. Sci. Lett., 146, 29–45, 1997.

Coynel, A., Seyler, P., Etcheber, H., Meybeck, M., and Orange, D.: Spatial and seasonal dynamics of total suspended sediment and organic carbon species in the Congo River, Global Biogeochem. Cy., 19, GB4019, doi:10.1029/2004GB002335, 2005.

de Abreu, L., Shackleton, N. J., Schönfeld, J., Hall, M., and Chapman, M.: Millennial-scale oceanic climate variability off the Western Iberian margin during the last two glacial periods, Mar. Geol., 196, 1–20, 2003.

deMenocal, P. B.: Plio-Pleistocene African climate, Science, 270, 53–59, 1995.

deMenocal, P., Ortiz, J., Guilderson, T., Adkins, J., Sarnthein, M., Baker, L., and Yarusinsky, M.: Abrupt onset and termination of the African Humid Period: rapid climate responses to gradual insolation forcing, Quaternary Sci. Rev., 19, 347–361, 2000.

Driessen, P. M., Deckers, J. A., Spaargaren, O. C., and Nachtergaele, F. O.: Lecture Notes on the Major Soils of the World. Food and Agriculture Organization of the United Nations, Rome, 2001.

Dupont, L. M. and Hooghiemstra, H.: The Saharan-Sahelian boundary during the Brunhes chron, Acta Bot. Neerl., 38, 405–415, 1989.

Eynaud, F., de Abreu, L., Voelker, A., Schönfeld, J., Salgueiro, E., Turon, J.-L., Penaud, A., Toucanne, S., Naughton, F., Sánchez Goñi, M. F., Malaizé, B., and Cacho, I.: Position of the Polar Front along the western Iberian margin during key cold episodes

of the last 45 ka, Geochem. Geophys. Geosyst., 10, Q07U05, doi:10.1029/2009GC002398, 2009.

FAO: Fighting sand enroachment: lessons from Mauritania, FAO Forestry Paper 158, Rome, 2010.

Gac, J. Y. and Kane, A.: Le fleuve Sénégal: I. Bilan hydrologique et flux continentaux de matières particulaires à l'embouchure, Sci. Géolog. Bull., 39, 99–130, 1986 (French).

Goudie, A. S. and Middleton, N. J.: Saharan dust storms: nature and consequences, Earth-Sci. Rev., 56, 179–204, 2001.

Govin, A., Holzwarth, U., Heslop, D., Ford Keeling, L., Zabel, M., Mulitza, S., Collins, J. A., and Chiessi, C. M.: Distribution of major elements in Atlantic surface sediments (36°N-49°S): Imprint of terrigenous input and continental weathering, Geochem. Geophys. Geosyst., 13, Q01013, doi:10.1029/2011GC003785, 2012.

Grousset, F. E., Parra, M., Bory, A., Martinez, P., Bertrand, P., Shimmield, G., and Ellam, R. M.: Saharan wind regimes traced by the Sr-Nd isotopic composition of subtropical Atlantic sediments: Last Glacial Maximum vs today, Quaternary Sci. Rev., 17, 395–409, 1998.

Grove, A. T.: The ancient erg of Hausaland, and similar formations on the south side of the Sahara, The Geographical Journal, 124, 528–533, 1958.

Grove, A. T. and Warren, A.: Quaternary landforms and climate on the south side of the Sahara, The Geographical Journal, 134, 194–208, 1968.

Hanebuth, T. J. J. and Henrich, R..: Recurrent decadal-scale dust events over Holocene western Africa and their control on canyon turbidite activity (Mauritania), Quaternary Sci. Rev., 28, 261–270, 2009.

Haynes Jr., C. V.: Bagnold's barchan: A 57-yr record of dune movement in the eastern Sahara and implications for dune origin and paleoclimate since Neolithic times, Quaternary Res., 32, 153–167, 1989.

Henrich, R., Cherubini, Y., and Meggers, H.: Climate and sea level induced turbidite activity in a canyon system offshore the hyperarid Western Sahara (Mauritania): The Timiris Canyon, Mar. Geol., 275, 178–198, 2010.

Hooghiemstra, H., Lézine, A.-M., Leroy, S. A. G., Dupont, L., and Marret, F.: Late Quaternary palynology in marine sediments: A synthesis of the understanding of pollen distribution patterns in the NW African setting, Quaternary Int., 148, 29–44, 2006.

Itambi, A. C., von Dobeneck, T., Mulitza, S., Bickert, T., and Heslop, D.: Millennial-scale northwest African droughts related to Heinrich events and Dansgaard-Oeschger cycles: Evidence in marine sediments from offshore Senegal, Paleoceanography, 24, PA1205, doi:10.1029/2007PA001570, 2009.

Jullien, E., Grousset, F., Malaizé, B., Duprat, J., Sanchez-Goni, M. F., Eynaud, F., Charlier, K., Schneider, R., Bory, A., Bout, V., and Flores, J. A.: Low-latitude "dusty events" vs. high-latitude "icy Heinrich events", Quaternary Res., 68, 379–386, 2007.

Just, J., Heslop, D., von Dobeneck, T., Bickert, T., Dekkers, M. J., Frederichs, T., Meyer, I., and Zabel, M.: Multiproxy characterization and budgeting of terrigenous end-members at the NW African continental margin, Geochem. Geophys. Geosyst., 13, Q0AO01, doi:10.1029/2012GC004148, 2012.

Kageyama, M., Mignot, J., Swingedouw, D., Marzin, C., Alkama, R., and Marti, O.: Glacial climate sensitivity to different states of the Atlantic Meridional Overturning Circulation: results from the IPSL model, Clim. Past, 5, 551–570, doi:10.5194/cp-5-551-2009, 2009.

Kim, J.-H., Schneider, R. R., Mulitza, S., and Muller, P. J.: Reconstruction of SE trade-wind intensity based on sea-surface temperature gradients in the Southeast Atlantic over the last 25 kyr, Geophys. Res. Lett., 30, 2144, doi:10.1029/2003GL017557, 2003.

Kocurek, G., Havholm, K. G., Deynoux, M. A. X., and Blakey, R. C.: Amalgamated accumulations resulting from climatic and eustatic changes, Akchar Erg, Mauritania, Sedimentology, 38, 751–772, 1991.

Kutzbach, J. E. and Liu, Z.: Response of the African monsoon to orbital forcing and ocean feedbacks in the middle Holocene, Science, 278, 440–443, 1997.

Lancaster, N., Kocurek, G., Singhvi, A., Pandey, V., Deynoux, M., Ghienne, J.-F., and Lo, K.: Late Pleistocene and Holocene dune activity and wind regimes in the western Sahara Desert of Mauritania, Geology, 30, 991–994, 2002.

Lézine, A.-M.: Late quaternary vegetation and climate of the Sahel, Quaternary Res., 32, 317–334, 1989.

Mahowald, N. M., Baker, A. R., Bergametti, G., Brooks, N., Duce, R. A., Jickells, T. D., Kubilay, N., Prospero, J. M., and Tegen, I.: Atmospheric global dust cycle and iron inputs to the ocean, Global Biogeochem. Cy., 19, GB4025, doi:10.1029/2004GB002402, 2005.

Marín, L., Forman, S. L., Valdez, A., and Bunch, F.: Twentieth century dune migration at the Great Sand Dunes National Park and Preserve, Colorado, relation to drought variability, Geomorphology, 70, 163–183, 2005.

Martrat, B., Grimalt, J. O., Shackleton, N. J., de Abreu, L., Hutterli, M. A., and Stocker, T. F.: Four Climate Cycles of Recurring Deep and Surface Water Destabilizations on the Iberian Margin, Science, 317, 502–507, 2007.

McManus, J. F., Francois, R., Gherardi, J. M., Keigwin, L. D., and Brown-Leger, S.: Collapse and rapid resumption of Atlantic meridional circulation linked to deglacial climate changes, Nature, 428, 834–837, 2004.

McTainsh, G.: Desert loess in northern Nigeria, Zeitschrift für Geomorphologie, 31, 145–165, 1987.

Meehl, G. A., Stocker, T. F., Collins, W. D., Friedlingstein, P., Gaye, A. T., Gregory, J. M., Kitoh, A., Knutti, R., Murphy, J. M., Noda, A., Raper, S. C. B., Watterson, I. G., Weaver, A. J., and Zhao, Z.-C.: Global Climate Projections, in: Climate Change 2007: The Physical Science Basis, edited by: Solomon, S., Qin, D., Manning, M., Chen, Z., Marquis, M., Averyt, K. B., Tignor, M., and Miller, H. L., Contribution of Working Group I to the Fourth Assessment Report of the Intergovernmental Panel on Climate Change. Cambridge University Press, Cambridge, United Kingdom and New York, NY, USA, 2007.

Michel, J., Westphal, H., and Hanebuth, T. J. J.: Sediment partitioning and winnowing in a mixed eolian-marine system (Mauritanian Shelf), Geo-Mar. Lett., 29, 221–232, 2009.

Michel, P.: Les bassins des fleuves Sénégal et Gambie, Etude géomorphologique, ORSTROM, Paris, 1973.

Miller, R. L. and Tegen, I.: Climate Response to Soil Dust Aerosols, J. Climate, 11, 3247–3267, 1998.

Mittelstaedt, E.: The upwelling area off Northwest Africa – a description of phenomena related to coastal upwelling, Proc. Oceanography, 12, 307–331, 1983.

Moreno, A., Cacho, I., Canals, M., Prins, M. A., Sánchez-Goñi, M. F., Grimalt, J. O., and Weltje, G. J.: Saharan dust transport and

high-latitude glacial climatic variability: the Alboran Sea record, Quaternary Res., 58, 318–328, 2002.

Moreno, T., Querol, X., Castillo, S., Alastuey, A., Cuevas, E., Herrmann, L., Mounkaila, M., Elvira, J., and Gibbons, W.: Geochemical variations in aeolian mineral particles from the Sahara–Sahel Dust Corridor, Chemosphere, 65, 261–270, 2006.

Muckersie, C. and Shepherd, M. J.: Dune phases as time-transgressive phenomena, Manawatu, New Zealand, Quaternary Int., 26, 61–67, 1995.

Mulitza, S., Prange, M., Stuut, J. B., Zabel, M., von Dobeneck, T., Itambi, A. C., Nizou, J., Schulz, M., and Wefer, G.: Sahel megadroughts triggered by glacial slowdowns of Atlantic meridional overturning, Paleoceanography, 23, PA4206, doi:10.1029/2008PA001637, 2008.

Mulitza, S., Heslop, D., Pittauerova, D., Fischer, H. W., Meyer, I., Stuut, J-B., Zabel, M., Mollenhauer, G., Collins, J. A., Kuhnert, H., and Schulz, M.: Increase in African dust flux at the onset of commercial agriculture in the Sahel region, Nature, 466, 226–228, 2010.

NGRIP: High-resolution record of Northern Hemisphere climate extending into the last interglacial period, Nature, 431, 147–151, 2004.

Niedermeyer, E. M., Prange, M., Mulitza, S., Mollenhauer, G., Schefuß, E., and Schulz, M.: Extratropical forcing of Sahel aridity during Heinrich stadials, Geophys. Res. Lett., 36, L20707, doi:10.1029/2009GL039687, 2009.

Niedermeyer, E. M., Schefuß, E., Sessions, A. L., Mulitza, S., Mollenhauer, G., Schulz, M., and Wefer, G.: Orbital- and millennial-scale changes in the hydrologic cycle and vegetation in the western African Sahel: insights from individual plant wax δD and δ^{13}C, Quaternary Sci. Rev., 29, 2996–3005, 2010.

Pierau, R., Henrich, R., Preiß-Daimler, I., Krastel, S., and Geersen, J.: Sediment transport and turbidite architecture in the submarine Dakar Canyon off Senegal, NW-Africa, J. Afr. Earth Sci., 60, 196–208, 2011.

Prospero, J. M. and Lamb, P. J.: African Droughts and Dust Transport to the Caribbean: Climate Change Implications, Science, 302, 1024–1027, 2003.

Prospero, J. M., Glaccum, R. A., and Nees, R. T.: Atmospheric transport of soil dust from Africa to South America, Nature, 289, 570–572, 1981.

Pye, K.: Processes of Fine Particle Formation, Dust Source Regions, and Climatic Changes, Paleoclimatology and Paleometeorology: Modern and Past Patterns of Global Atmospheric Transport, NATO ASI Series, 282, 3–30, 1989.

Pye, K.: The nature, origin and accumulation of loess, Quaternary Sci. Rev., 14, 653–667, 1995.

Rea, D. K.: The paleoclimatic record provided by eolian deposition in the deep sea: The geologic history of wind, Rev. Geophys., 32, 159–195, 1994.

Rosenfeld, D., Rudich, Y., and Lahav, R.: Desert dust suppressing precipitation: A possible desertification feedback loop, Proc. Natl. Acad. Sci. USA, 98, 5975–5980, 2001.

Salgueiro, E., Voelker, A. H. L., de Abreu, L., Abrantes, F., Meggers, H., and Wefer, G.: Temperature and productivity changes off the western Iberian margin during the last 150 ky, Quaternary Sci. Rev., 29, 680–695, 2010.

Salzmann, U. and Waller, M.: The Holocene vegetational history of the Nigerian Sahel based on multiple pollen profiles, Rev.

Palaeobot. Palynol., 100, 39–72, 1998.

Sarnthein, M. and Diester-Haass, L.: Eolian-sand turbidites, J. Sediment. Res., 47, 868–890, 1977.

Sarnthein, M., Tetzlaff, G., Koopmann, B., Wolter, K., and Pflaumann, U.: Glacial and interglacial wind regimes over the eastern subtropical Atlantic and North-West Africa, Nature, 293, 193–196, 1981.

Servant, M.: Séquences continentales et variations climatiques: évolution du bassin du Tchad au Cénozoique supérieur, Travaux et Documents de l'ORSTOM 159, 1983.

Skonieczny, C., Bory, A., Bout-Roumazeilles, V., Abouchami, W., Galer, S. J. G., Crosta, X., Stuut, J-B., Meyer, I., Chiapello, I., Podvin, T., Chatenet, B., Diallo, A., and Ndiaye, T.: The 7-13 March 2006 major Saharan outbreak: Multiproxy characterization of mineral dust deposited on the West African margin, J. Geophys. Res., 116, D18210, doi:10.1029/2011JD016173, 2011.

Stuut, J.-B., Zabel, M., Ratmeyer, V., Helmke, P., Schefuß, E., Lavik, G., and Schneider, R.: Provenance of present-day eolian dust collected off NW Africa, J. Geophys. Res., 110, D04202, doi:10.1029/2004JD005161, 2005.

Svensson, A., Andersen, K. K., Bigler, M., Clausen, H. B., Dahl-Jensen, D., Davies, S. M., Johnsen, S. J., Muscheler, R., Parrenin, F., Rasmussen, S. O., Röthlisberger, R., Seierstad, I., Steffensen, J. P., and Vinther, B. M.: A 60 000 year Greenland stratigraphic ice core chronology, Clim. Past, 4, 47–57, doi:10.5194/cp-4-47-2008, 2008.

Swezey, C.: Eolian sediment responses to late Quaternary climate changes: temporal and spatial patterns in the Sahara, Palaeogeogr. Palaeocli., 167, 119–155, 2001.

Talbot, M. R.: Environmental responses to climatic change in the West African Sahel over the past 20 000 years, in: The Sahara and the Nile, edited by: Williams, M. A. J. and Faure, H., Quaternary environments and prehistoric occupation in northern Africa. A. A. Balkema, Rotterdam, 37-62, 1980.

Tjallingii, R., Claussen, M., Stuut, J.-B.W., Fohlmeister, J., Jahn, A., Bickert, T., Lamy, F., and Rohl, U.: Coherent high- and low-latitude control of the northwest African hydrological balance, Nat. Geosci., 1, 670–675, 2008.

Watrin, J., Lézine, A.-M., and Hély, C.: Plant migration and plant communities at the time of the "green Sahara", Comp. Rendus Geoscie., 341, 656–670, 2009.

Wefer, G. and Fischer, G.: Seasonal pattern of vertical particle flux in equatorial and coastal upwelling areas of the eastern Atlanctic, Deep Sea Res., 40, 1613–1645, 1993.

Weldeab, S., Lea, D. W., Schneider, R. R., and Andersen, N.: 155,000 years of West African monsoon and ocean thermal evolution, Science, 316, 1303–1307, 2007.

Weltje, G. J. and Tjallingii, R.: Calibration of XRF core scanners for quantitative geochemical logging of sediment cores: Theory and application, Earth Planet. Sci. Lett., 274, 423–438, 2008.

Zarriess, M. and Mackensen, A.: The tropical rainbelt and productivity changes off northwest Africa: A 31,000-year high-resolution record, Mar. Micropaleontol., 76, 76–91, 2010.

Zarriess, M., Johnstone, H., Prange, M., Steph, S., Groeneveld, J., Mulitza, S., and Mackensen, A.: Bipolar seesaw in the northeastern tropical Atlantic during Heinrich stadials, Geophys. Res. Lett., 38, L04706, doi:10.1029/2010GL046070, 2011.